A p85α–osteopontin axis couples the ICOS receptor to sustained Bcl-6 expression by follicular helper and regulatory T cells

HHS Public Access

Author manuscript

Nat Immunol. Author manuscript; available in PMC 2015 July 01.

Published in final edited form as:

Nat Immunol. 2015 January ; 16(1): 96–106. doi:10.1038/ni.3050.

A p85α–osteopontin axis couples the ICOS receptor to sustained Bcl-6 expression by follicular helper and regulatory T cells

Jianmei W. Leavenworth[1,2], **Bert Verbinnen**[1,2], **Jie Yin**[1,3], **Huicong Huang**[1,4], and **Harvey Cantor**[1,2]

[1]Department of Cancer Immunology and AIDS, Dana-Farber Cancer Institute, Boston, MA 02115 USA

[2]Department of Microbiology & Immunobiology, Division of Immunology, Harvard Medical School, Boston, MA 02115 USA

[3]Department of Cell Biology, School of Basic Medical Sciences, Tianjin Medical University, Tianjin, 300070 PR China

[4]Department of Parasitology, Wenzhou Medical College, Wenzhou, Zhejiang, 325035 PR China

Abstract

Follicular helper T (T_{FH}) cells and follicular regulatory T (T_{FR}) cells regulate the quantity and quality of humoral immunity. Although both cell types highly express the co-stimulatory receptor ICOS and require the transcription factor Bcl-6 for their differentiation, the ICOS-dependent pathways that coordinate their responses are not well understood. Here we report that ICOS activation in $CD4^+$ T cells promotes the interaction of the p85α regulatory subunit of the signaling kinase PI3K and intracellular osteopontin (OPN-i), followed by nuclear translocation of OPN-i, interaction with Bcl-6 and protection of Bcl-6 from ubiquitin-dependent proteasome degradation. Post-translational protection of Bcl-6 expression by OPN-i is essential for sustained T_{FH} and T_{FR} cell responses and regulation of the germinal center B cell response to antigen. As such, the p85α–OPN-i axis represents a molecular bridge that couples ICOS activation to Bcl-6-dependent functional differentiation of T_{FH} and T_{FR} cells and suggests new therapeutic avenues to manipulate their responses.

The generation of long-lived high-affinity antibodies after microbial infection or vaccine induction requires precise control of the germinal center (GC) reaction. Follicular helper T (T_{FH}) cells are specialized effector $CD4^+$ T cells that provide help for GC formation and

---

Correspondence: Harvey Cantor, 450 Brookline Avenue, Boston, MA 02115 USA; 617 632 3348; 617 632 4630 fax; Harvey_Cantor@dfci.harvard.edu.

Accession Codes. GEO: Microarray data have been deposited under accession number GSE61284.

Author Contributions

JWL and HC conceived and planned experiments; BV made the OPN-i KI genomic construct; JWL, JY and HH performed experiments; JWL and HC analyzed data and wrote the paper.

Competing financial interests

The authors declare no competing financial interests.

induce GC B cells to develop protective antibody responses to invading pathogens. Bcl-6, a proto-oncoprotein and transcriptional repressor belonging to the BTB-POZ family, has been identified as the central transcription factor that controls T_{FH} differentiation and associated GC responses [1–3]. Because Bcl-6 deficiency can result in increased susceptibility to chronic infection, while its excessive expression is associated with autoimmunity and lymphocytic transformation, precise control of Bcl-6 expression during T cell differentiation represents an essential component of the T_{FH} cell response [4]. Moreover, recently-defined $Foxp3^+$ follicular regulatory T cells (T_{FR}) that inhibit GC responses also require Bcl-6 expression for their differentiation and suppressive activity [5–7]. However, in contrast to our insight into the molecular elements that regulate Bcl-6 expression in GC B cells [4], the mechanisms that govern Bcl-6 expression by both T_{FH} and T_{FR} cells are poorly understood.

The differentiation of T_{FH} cells *in vivo* can be divided into several stages that include initiation, maintenance and full polarization [8]. This process depends on early upregulation of *Bcl-6* gene expression during T-cell activation and T_{FH} commitment, followed by continued enhanced Bcl-6 expression during the maintenance and polarization phases of the T_{FH} cell response [9]. Although engagement of the ICOS receptor represents a key event in a process that culminates in Bcl-6 expression and acquisition of the T_{FH} and T_{FR} phenotypes, the essentials of this specialized inductive pathway have not been clarified.

ICOS binding its ligand (ICOSL) expressed by antigen-presenting cells (APC) results in recruitment of the phosphatidylinositol-3-OH kinase (PI3K) signaling complex that consists of a regulatory p85α subunit and a catalytic p110 component. Recruitment of PI3K to ICOS is an essential step in T_{FH} cell differentiation, as mutations of the ICOS cytoplasmic tail that abrogate recruitment of PI3K impair T_{FH} cell generation and GC responses [10]. Although deficient expression of the p110δ component impairs follicular migration of T_{FH} cells [11, 12], ICOS-dependent upregulation of Bcl-6 expression and development of $CXCR5^+$ T_{FH}-like cells proceed normally [11–13]. In contrast, the contribution of the p85α component of PI3K to Bcl-6 expression and development of both T_{FH} and T_{FR} cells remains unclear. Because p85α regulates the activity and localization of intracellular proteins [14–16], we asked whether an interaction between p85α and downstream intracellular protein(s) in $CD4^+$ T cells after ICOS stimulation might contribute to the Bcl-6-dependent T_{FH} and T_{FR} cell program.

The phosphoprotein osteopontin (OPN, encoded by *Spp1*) is expressed in activated T cells [17–23]. Although dysregulated expression of OPN has been associated with a broad spectrum of T_{FH}-associated autoimmune diseases and strongly correlates with autoantibody production [17–23], the precise contribution of OPN to T_{FH} cell differentiation is uncertain. OPN is expressed as either a secreted (OPN-s) or intracellular (OPN-i) isoform that results from differential usage of *Spp1* translational initiation sites [17]. To clarify the contribution of each OPN isoform to the regulation of T_{FH} responses, here we generated knock-in mice that expressed only OPN-i and compared them with wild-type mice that express both isoforms or OPN knockout (KO) mice that express neither OPN isoform. We find that OPN-i functions as a positive regulator of both T_{FH} and T_{FR} cell differentiation by enhancing Bcl-6 protein stability, and we identify the p85α–OPN-i complex as a critical molecular bridge that couples ICOS engagement to sustained T_{FH} and T_{FR} responses that combine to regulate the GC antibody response.

Results

Expression of OPN-i is essential for T_{FH} and T_{FR} cell differentiation

We first analyzed OPN mRNA and protein expression in different $CD4^+$ T cell subsets after immunization with keyhole limpet hemocyanin (KLH) precipitated in complete Freund's adjuvant (CFA). We noted that OPN was expressed most abundantly by the $CD4^+$ T_{FH} and T_{FR} subsets compared with other $CD4^+$ T cell subsets (Fig. 1a and Supplementary Fig. 1), suggesting a potential contribution of OPN to the development of these follicular effector and regulatory T cells.

To define the contribution of OPN isoforms, we generated mice bearing a *Spp1*^{flstop} allele knocked into the *Spp1* locus. In this system, Cre/*lox*P-mediated recombination induces expression of the OPN-i isoform [17] after excision of a STOP cassette (Supplementary Fig. 2a). Crossing of *Spp1*^{flstop} mice with EIIa-Cre mice, which express the Cre recombinase from the adenovirus EIIa promoter during embryonic development, generated *Spp1*^{flstop} Cre^+ (hereafter OPN-i KI), which express intracellular OPN), and the *Spp1*^{flstop} Cre^- mice (hereafter OPN KO), which do not express either OPN-i or OPN-s. Both genotypes were developmentally indistinguishable from wild-type littermates and PCR analysis confirmed expression of the *Spp1*^{flstop} alleles at the *Spp1* locus (Supplementary Fig. 2b). Secreted OPN was not detectable in supernatants of freshly isolated or activated T cells, DC, macrophages or NK cells from either OPN-i KI or OPN KO mice (Supplementary Fig. 2c). Moreover, immunoblot analysis showed equivalent intracellular expression of OPN protein in unfractionated splenocytes from OPN-i KI and OPN wild-type mice (Supplementary Fig. 2d). Expression of OPN-i, but not OPN-s, by plasmacytoid dendritic cells (pDC) is essential for efficient production of IFN-α after Toll-like receptor ligation [21]. As an additional control, activated pDC from OPN-i KI and wild-type mice expressed similar levels of IFN-α, while pDC from OPN KO mice expressed no IFN-α (Supplementary Fig. 2e), confirming the functional phenotype of OPN-i KI mice.

We next investigated the contribution of OPN-i to T_{FH} and T_{FR} cell differentiation by comparing OPN-i KI mice with transgenic expression of the OT-II ovalbumin (OVA)-specific T cell antigen receptor (TCR) to OT-II and OT-II OPN KO mice. These mice were immunized with 4-hydroxy-3-nitrophenyl linked to OVA (NP_{13}-OVA) to induce antigen-specific $CD4^+$ T cell responses. Total and high-affinity antibody responses were reduced by 80–90% in OT-II OPN KO mice compared with OT-II mice (Fig. 1b), while antibody titers in OT-II OPN-i KI mice were similar to OT-II mice. Although T cell activation was not obviously impaired in OT-II OPN KO mice compared to OT-II and OT-II OPN-i KI mice as judged from CD44 expression (Supplementary Fig. 3a), OT-II OPN KO mice displayed defective formation of T_{FH} cells, T_{FR} cells (but not $Foxp3^+$ T_{reg}) and GC B cells (Fig. 1c, d and Supplementary Fig. 3a). These findings suggest that expression of OPN-i is essential for both T_{FH} and T_{FR} cell formation and for T_{FH}-associated high-affinity antibody responses.

OPN-i specifically promotes T_{FH} cell differentiation

To address if the requirement for OPN expression is cell intrinsic to the T_{FH} cells, we transferred OT-II OPN KO $CD4^+$ T cells together with wild-type B cells into

Rag2$^{-/-}$*Prf1*$^{-/-}$ hosts, which are defective in T and B cells and lack perforin activity in NK cells, followed by immunization with NP_{13}-OVA. We noted substantially reduced serum anti-NP total IgG and IgG1 and diminished splenic T_{FH} and GC B cell formation in *Rag2*$^{-/-}$*Prf1*$^{-/-}$ hosts reconstituted with OT-II OPN KO CD4$^+$ T cells compared to the response of mice reconstituted with OT-II OPN-i KI or OT-II CD4$^+$ T cells (Fig. 2a, b). When co-transferred with wild-type CD4$^+$ T cells into *Rag2*$^{-/-}$*Prf1*$^{-/-}$ hosts, OPN KO and wild-type B cells produced equivalent antibody responses suggesting OPN is not required in B cells for antibody production (Supplementary Fig. 3b). In addition, we analyzed OT-II OPN KO CD4$^+$ T cells compared to OT-II OPN-i KI and OT-II CD4$^+$ T cells after transfer into wild-type CD45.1 congenic mice that were immunized with OVA in CFA. Despite normal expansion and activation of OT-II OPN KO CD4$^+$ T cells, according to numbers of $V_\beta5^+$ CD4 cells and expression of CD44 (Supplementary Fig. 3c), donor OT-II OPN KO CD4$^+$ T cells displayed reduced CXCR5$^+$ T_{FH} cell frequency and expression of intracellular IL-21 compared to OT-II OPN-i KI and OT-II counterparts (Supplementary Fig. 3d). In contrast, the frequency of $V_\beta5^+$ CD4$^+$ T cells expressing IFNγ, IL-4, and IL-17A, corresponding to T_H1, T_H2 and T_H17 subsets respectively, was not reduced in OT-II OPN KO CD4 cells (Supplementary Fig. 3d). When differentiated *in vitro* in T_H polarizing conditions, naïve OT-II OPN KO CD4$^+$ T cells showed slightly increased differentiation into IL-17-producing cells compared to OT-II OPN-i KI and OT-II CD4$^+$ T cells, while there was a modest, but not significant decrease in IFNγ expression by OT-II OPN KO CD4$^+$ T cells compared to OT-II OPN-i KI and OT-II counterparts (Supplementary Fig. 3e). In addition, OPN KO CD4$^+$ T cells differentiated into induced T_{reg} (iT_{reg}) cells with similar suppressive activity compared with wild-type and OPN-i KI CD4$^+$ T cells (Supplementary Fig. 4a, b). These results suggest that OPN-i specifically promotes T_{FH} cell differentiation and is not required for T_H1, T_H2, T_H17 or iT_{reg} cell differentiation.

OPN-i expression in T_{reg} cells is required for T_{FR} cell differentiation

T_{FR} cells originate from CXCR5$^-$Foxp3$^+$ natural T_{reg} cells and are characterized as PD1$^+$CXCR5$^+$Foxp3$^+$ T cells [6, 7]. To determine whether OPN-i promotes T_{FR} cell formation, we co-transferred CD45.1$^+$ CD4$^+$ naïve T cells (sorted as CD25$^-$GITR$^-$CD44^{lo}CD62L^{hi}) with CD45.2$^+$CD4$^+$ T_{reg} cells (sorted as CD25^{hi}CD44^{int}CXCR5$^-$) from either wild-type, OPN KO or OPN-i KI mice at a ratio of 2:1 into *Tcr*α$^{-/-}$ hosts, followed by immunization with NP_{26}-KLH in CFA. We observed a significant reduction of OPN KO CD45.1$^-$PD1$^+$CXCR5$^+$Foxp3$^+$CD4$^+$ T_{FR} cells 10 d post-immunization (Fig. 2c, d), which was associated with increased GC B cell formation (Fig. 2c, d) as well as anti-NP (Supplementary Fig. 4c) and anti-KLH antibody titers (Supplementary Fig. 4d) in recipients of OPN KO CD4$^+$ Treg, compared with the response after transfer of wild-type and OPN-i KI CD4$^+$ T_{reg} cells. These results suggest that OPN-i-deficiency impairs T_{FR} cell differentiation from CXCR5$^-$ T_{reg} precursors.

Transfer of differentiated OPN KO T_{FR} cells along with wild-type B cells into *Rag2*$^{-/-}$*Prf1*$^{-/-}$ hosts followed by NP_{26}-KLH immunization resulted in greater expansion of GL7$^+$Fas$^+$ GC B cells and higher amounts of NP-specific total and high-affinity IgG compared to hosts transferred with the same numbers of OPN-i KI T_{FR} cells (Fig. 2e–g and Supplementary Fig. 1), suggesting that OPN-i deficiency diminishes T_{FR} suppressive

activity on a per-cell basis *in vivo*. Transfer of mixtures of T_{FH} cells and T_{FR} cells at different ratios (2:1, 1:1 and 0.5:1) with wild-type B cells into *Rag2*$^{-/-}$*Prf1*$^{-/-}$ hosts followed by NP_{26}-KLH immunization showed increased serum anti-NP total IgG in hosts transferred with higher numbers of T_{FH} cells, suggesting that the magnitude of T_{FR} cell-mediated suppression is dependent on the extent of T_{FH}-driven antibody responses (Fig. 2g). Taken together these results indicate that OPN-i expression is required for the generation of functional T_{FR} cells.

OPN-i deficiency impairs Bcl-6 protein expression

Because the transcription factor Bcl-6 is critical for T_{FH} and T_{FR} cell differentiation [6–8], we asked whether the impaired follicular T cell response of OPN KO CD4$^+$ T cells was associated with reduced Bcl-6 expression. Flow cytometry and immunoblot analysis of Bcl-6 expression during T_{FH} cell development *in vivo* in wild-type mice showed that Bcl-6 was detectable by day 1, peaked at day 7.5 and waned by day 10 after KLH immunization (Fig. 3a, b and Supplementary Fig. 1, 4e), consistent with a previous study [24]. Expression of Bcl-6 in T_{FR} cells followed a similar kinetic, albeit expression was lower than in T_{FH} cells (Fig. 3a, b). OPN deficiency did not alter *Bcl-6* and *Prdm1* mRNA expression and did not impair early Bcl6 protein expression by OPN KO CD4$^+$ T cells (within ~2 days), (Fig. 3a, b and Supplementary Fig. 4e, f). The OPN deficient response was marked by reduced generation of T_{FH} and T_{FR} cells by OPN KO CD4$^+$ T cells and severely decreased expression of Bcl-6 protein in the few residual OPN KO T_{FH} and T_{FR} cells by day 3 and thereafter (Fig. 3a–d). These findings suggest that although OPN-i does not regulate *Bcl-6* transcription, it may differentially affect expression of the Bcl-6 protein during differentiation into T_{FH} and T_{FR} cells.

ICOS co-stimulation promotes an interaction between OPN-i and p85α

ICOS co-stimulation is essential for the induction and maintenance of Bcl-6 expression during T_{FH} cell differentiation and is required for T_{FR} cell formation [5, 25, 26]. Because expression of OPN-i and Bcl-6 followed similar kinetics in T_{FH} and T_{FR} cells (Fig. 3e) and Bcl-6 protein expression was reduced in the few CXCR5$^+$PD-1$^+$ T_{FH} cells generated in the OPN KO mice we tested the possibility that OPN-i mediates ICOS-induced Bcl-6 expression. Gene profile analysis (GSE61284) in CD4$^+$ T cells 8 h after CD3 and ICOS ligation identified ~210 genes, including OPN (*Spp1*), that were significantly ($P < 0.01$) upregulated compared to CD3 ligation alone (Supplementary Fig. 5a). Pathway analysis (Ingenuity®) of these genes revealed that they were involved with many biological functions associated with T cell activation, antibody production and with systemic autoimmune disease (Supplementary Fig. 5b, c). We confirmed *Spp1* mRNA and OPN protein upregulation by ICOS and CD3 co-stimulation compared to CD3 ligation alone in *in vitro*-activated CD4$^+$ T cells (Fig. 4a, b). *Icos*$^{-/-}$ CD4$^+$ T cells did not upregulate expression of OPN and Bcl-6 proteins compared with wild-type CD4$^+$ T cells after KLH immunization (Fig. 4c). Impaired upregulation of OPN and Bcl-6 proteins was also observed in effector CD25$^-$CD44^{hi}GITR$^-$CD4$^+$ T cells and regulatory CD25$^+$CD44^{hi}GITR$^+$CD4$^+$ T cells from OT-II *Icos*$^{-/-}$ mice after OVA immunization (Fig. 4d). These findings suggest that ICOS ligation regulates OPN-i expression in *in vivo*-activated CD4$^+$ T cells.

Because activation of the PI3K signaling pathway is induced by ICOS ligation [10], we determined whether OPN-i associates with the p110-p85 components of the PI3K complex. OPN-i did not interact with the p110α or p110δ subunits of PI3K in 293T cells transfected with plasmids encoding these proteins (Supplementary Fig. 6a, b). In addition, PI3K–Akt activation, as indicated by Akt phosphorylation, was not reduced in OPN KO $CD4^+$ T cells stimulated with anti-CD3 and anti-ICOS compared to OPN-i KI $CD4^+$ T cells (Supplementary Fig. 6c). Activation of IL-6 signals, as indicated by STAT1 and STAT3 phosphorylation, was also not impaired in OPN KO $CD4^+$ T cells after incubation with IL-6 compared to OPN-i KI controls (Supplementary Fig. 6d). However, overexpressed OPN-i co-immunoprecipitated with Flag-p85α in transfected 293T cell lines (Fig. 4e). In $CD4^+$ T cells stimulated with anti-CD3, endogenous OPN-i interacted with p85α in $CD4^+$ T cells and co-ligation of TCR and ICOS substantially increased their association (Fig. 4f), suggesting that ICOS-dependent activation promotes the interaction between p85α and OPN-i.

p85α is required for T_{FH} and T_{FR} cell differentiation

To determine whether p85α is required for Bcl-6 upregulation during T_{FH} cell differentiation we used mice with *lox*P-flanked alleles encoding p85α (*Pi3kr1*^{fl}) deleted by Cre recombinase expressed from the hematopoietic cell-specific *Vav1* promoter (*Pi3kr1*^{fl}Vav1-Cre^+), termed p85α KO mice here. After immunization of p85α KO mice with KLH in CFA ×3d, development of T_{FH} and T_{FR} cells as well as Bcl-6 expression in these cells was impaired in p85α KO mice compared to p85α wild-type mice (*Pi3kr1*^{fl}Vav1-Cre^-) (Supplementary Fig. 6e). To specifically analyze the contribution of p85α to T_{FH} cell differentiation, we transferred wild-type or p85α KO naïve $CD4^+$ T cells together with wild-type B cells into *Rag2*$^{-/-}$*Prf1*$^{-/-}$ hosts immunized with NP_{26}-KLH in CFA. Despite the nearly normal expansion and activation of transferred p85α KO $CD4^+$ T cells following immunization (Supplementary Fig. 6f), the frequency of p85α KO Bcl-6^+CXCR5^+Foxp$3^-$$CD4^+$ T_{FH} cells was greatly reduced and anti-NP antibody responses were impaired in adoptive hosts compared to hosts transferred with p85α wild-type $CD4^+$ T cells (Fig. 5a and Supplementary Fig. 6g). Loss of p85α in transferred $CD4^+$ T cells did not significantly alter their differentiation into T_H1, T_H2 and T_H17 cells *in vivo* (Supplementary Fig. 6h). However, p85α deficiency significantly impaired T_{FR} cell formation after co-transfer of p85α KO ($CD45.2^+$) $CD4^+$ T_{reg} cells with wild-type ($CD45.1^+$) naïve $CD4^+$ T cells into *Tcr*α$^{-/-}$ hosts immunized with NP_{26}-KLH in CFA. Recipients of p85α KO $CD4^+$ T_{reg} produced increased amounts of total and high-affinity anti-NP antibodies compared with recipients of p85α wild-type $CD4^+$ T_{reg} cells (Fig. 5b and Supplementary Fig. 6g). Taken together these results indicate that p85α is required for T_{FH} and T_{FR} cell formation.

To determine whether defective p85α expression diminished Bcl-6 expression, we transduced p85α KO $CD4^+$ T cells with retroviral vector expressing green fluorescent protein (GFP) alone (empty vector) or GFP and a constitutively-active form of Akt [27], then sorted GFP^+ cells and transferred them along with wild-type B cells into *Rag2*$^{-/-}$*Prf1*$^{-/-}$ hosts, followed by immunization with NP_{26}-KLH in CFA (Fig. 5c, d). Among the GFP^+ p85α KO $CD4^+$ T cells, more cells transduced with the constitutively active Akt (~14%) expressed phosphorylated Akt compared to cells transduced with the empty vector (2%; Fig.

5c). However, constitutively active Akt expression did not significantly increase expression of Bcl-6 and CXCR5 in p85α KO CD4$^+$ Tcells compared to cells infected with a control virus (Fig. 5d and Supplementary Fig. 6g). These findings indicate that PI3K-p85α but not PI3K-p110 is required for Bcl-6-dependent T_{FH} cell differentiation.

p85α chaperones nuclear translocation of OPN-i

Because the above findings suggested that p85α and OPN-i might contribute to Bcl-6-dependent T_{FH} cell differentiation, we sought to further define the interaction between p85α and OPN-i. In transfected 293T cells, the p85α-bound fraction of OPN underwent a shift in migration after treatment with protein phosphatases (Supplementary Fig. 6i), consistent with reports that p85α can recognize phosphorylated proteins. Using a web-based program (Scansite) [28, 29] we identified a sequence in the OPN protein near position Tyr 166 (UniProtKB: P10923) that might mediate an interaction with the SH2 domain of p85α (Supplementary Fig. 6j). Binding of a Y166F OPN-i mutant protein to p85α was substantially reduced compared to that of wild-type OPN-i protein (Fig. 6a), suggesting that interaction of p85α with OPN-i requires an intact OPN-i Y166 site.

We next examined the cellular localization of OPN protein in CD44$^+$CD4$^+$ T cells enriched from OPN-i KI mice 3d post-immunization with KLH in CFA. Confocal microscopic analysis revealed that Bcl-6 protein stained with anti-Bcl-6 before labeling with a secondary fluorescence antibody was mainly nuclear in Bcl-6$^+$ cells (representing ~10% of CD44$^+$CD4$^+$ T cells) and *in vitro* anti-ICOS restimulation further increased the abundance of intranuclear Bcl-6 (Fig. 6b and Supplementary Fig. 6k). While prior to ICOS stimulation OPN-i protein was located mainly in the cytosol of Bcl-6$^+$CD4$^+$ T cells, ICOS ligation caused most OPN-i protein to migrate within the nucleus (Fig. 6b, c). Because p85α can function as a chaperone to facilitate nuclear translocation of associated partner proteins [15, 16], we asked whether p85α assists in the nuclear translocation of OPN-i. In co-transfection experiments in 293T cells, nuclear accumulation of OPN-i increased in direct proportion to the amount of p85α (Fig. 6d), and OPN did not relocate to the nucleus following ligation of ICOS in p85α KO CD4$^+$ T cells (Fig. 6e). In addition, the OPN-i Y166F mutant protein remained mainly in the cytosol despite co-transfection with increased concentrations of p85α (Fig. 6d and Supplementary Fig. 7a). These findings suggest that the nuclear translocation of OPN-i is facilitated by a specific interaction of p85α and OPN-i.

Intranuclear OPN-i interacts with and stabilizes Bcl-6 expression

To characterize the potential interaction between OPN-i and Bcl-6, we immunoprecipitated Bcl-6 from $V_\beta5^+$ CD4$^+$ T cells purified from OT-II and OT-II OPN-i KI mice post-immunization with OVA in CFA. Staining for endogenous OPN-i protein in the Bcl-6 immunoprecipitates indicated that the two proteins interacted (Fig. 7a). Cellular fractionation revealed that the majority of Bcl-6–OPN-i complexes were found in the nucleus (Supplementary Fig. 7b), consistent with the results of confocal microscopic analysis (Supplementary Fig. 7a). To specifically analyze the sequences of Bcl-6 required for interaction with OPN-i, we constructed Bcl-6 protein deletion mutants, including deletion of sequences in BTB, PEST or Zinc finger domains of Bcl-6 (Supplementary Fig. 7c). Co-immunoprecipitation analysis of overexpressed OPN-i and Flag–Bcl-6 wild-type or

mutants in 293T cells indicated that sequences in RD2 of Bcl-6 (amino acids 120–300), but not the BTB, PEST or Zinc finger domains of Bcl-6 were required for interaction with OPN-i (Fig. 7b and Supplementary Fig. 7c, d). These findings indicate that intranuclear OPN-i may interact with Bcl-6.

Because OPN KO CD4$^+$ T_{FH} and T_{FR} cells expressed less Bcl-6 protein at day 3 to 10 post-KLH-immunization, we next tested if the absence of OPN-i rendered the Bcl-6 protein unstable. Addition of cycloheximide (CHX), which inhibits protein synthesis, into cultures of OT-II CD4$^+$ T cells purified from OT-II OPN KO mice 2.5 d after OVA-immmunization followed by *in vitro* anti-CD3 and anti-ICOS stimulation, resulted in more reduction of Bcl-6 protein (90%) compared to OT-II and OT-II OPN-i KI CD4$^+$ T cells (50%) (Fig. 7c). In addition, overexpression of OPN-i prolonged the stability of Bcl-6 protein in CHX-treated 293T cell lines (Fig. 7d). Reduced Bcl-6 amounts in all these CHX-treated CD4$^+$ T cells were rescued by the addition of the proteasome inhibitor MG132 (Fig. 7c), suggesting loss of Bcl-6 was proteasome-dependent. Moreover, MG132 treatment resulted in the appearance of high molecular mass species of Bcl-6 in the denatured extracts of these cells (Fig. 7e, f). These high molecular forms of Bcl-6 were increased in the presence of overexpressed ubiquitin (Fig. 7e, f) suggesting they were ubiquitinated forms of Bcl-6. Addition of a pan deubiquitination inhibitor (DUbi) accelerated Bcl-6 degradation in wild-type, OPN KO and OPN-i KI CD4$^+$ T cells as well as Flag–Bcl-6-transfected 293T cells. This effect was substantially prevented by endogenous expression of OPN-i by wild-type and OPN-i KI CD4$^+$ T cells and overexpressed OPN-i in 293T cells (Fig. 7g and Supplementary Fig. 7e). These results suggest that OPN-i stabilizes Bcl-6 through interference with ubiquitin-mediated degradation of Bcl-6.

The p85α–OPN-i interaction regulates T_{FH} and T_{FR} responses *in vivo*

To test the physiological relevance of the p85α–OPN-i interaction in T_{FH} differentiation, we transduced OT-II OPN-i KI CD4$^+$ T cells with retroviral vector expressing GFP alone (empty vector) or GFP and either OPN-i wild-type or OPN-i Y166F mutant and co-transferred each with wild-type B cells into *Rag2*$^{-/-}$*Prf1*$^{-/-}$ hosts followed by immunization with NP_{13}-OVA in CFA. OT-II OPN KO CD4$^+$ T cells transduced with empty vector were included as controls. T_{FH} cell differentiation and intracellular expression of Bcl-6 in these T_{FH} cells assessed by flow cytometry were substantially increased in OT-II OPN-i KI CD4$^+$ T cells transduced with OPN-i wild-type compared to empty vector controls (Fig. 8a, b). Expression of the OPN-i Y166F in OT-II OPN-i KI CD4$^+$ T cells markedly decreased Bcl-6 expression and T_{FH} cell differentiation compared to these cells expressing the GFP alone (Fig. 8a, b) and to levels similar to those observed in OT-II OPN KO CD4$^+$ T cells transduced with empty vector (Fig. 8a, b). Similar results were obtained in a model in which CD4$^+$ T cells from wild-type or OPN KO mice immunized with type II collagen (CII) were transduced with retroviral vectors (as described above), transferred with wild-type B cells into *Rag2*$^{-/-}$*Prf1*$^{-/-}$ hosts followed by immunization with CII in CFA. Expression of OPN-i Y166F in wild-type CII-immune CD4$^+$ T cells decreased the differentiation of the collagen-specific T cells into Bcl-6$^+$ T_{FH} cells and reduced the frequency of GL7$^+$ B cells and autoantibody responses to collagen to levels observed in OPN KO CD4$^+$ T cells

expressing empty vector (Fig. 8c). These results suggest that interaction between OPN-i and p85α is essential for Bcl-6-dependent functional differentiation of T_{FH} cells.

Using a similar retroviral reconstitution system, we also evaluated the physiologic importance of the p85α–OPN-i interaction in the formation of T_{FR}. CD45.2$^+$ OPN KO CD25$^+$CD4$^+$ T cells were transduced with retroviral vectors expressing GFP alone (empty vector) or GFP and either OPN-i wild-type or OPN-i Y166F mutant and co-transferred with CD45.1$^+$ CD25$^-$CD4$^+$ T cells and wild-type B cells into *Rag2*$^{-/-}$*Prf1*$^{-/-}$ hosts, followed by immunization with NP_{26}-KLH in CFA. CD45.2$^+$ OPN-i KI CD25$^+$CD4$^+$ T cells transduced with empty vector were included as controls. Expression of wild-type OPN-i in OPN-KO CD25$^+$CD4$^+$ T cells markedly increased TFR differentiation to levels similar to that of OPN-i-KI CD25$^+$CD4$^+$ T cells expressing GFP alone (Fig. 8d). In contrast, expression of OPN-i Y166F in OPN-KO CD25$^+$CD4$^+$ T cells resulted in a substantially reduced frequency of Foxp3$^+$Bcl-6$^+$CXCR5$^+$ TFR cells and an increase in GC B cells and the titers of anti-NP and antinuclear antibody (Fig. 8d,e). Decreased T_{FR} cell formation was associated with an increase in GC B cell frequencies and markedly increased anti-NP and anti-ANA antibody titers in hosts transferred with OPN KO CD25$^+$CD4$^+$ T cells expressing OPN-i Y166F (Fig. 8d, e). Taken together, these results indicate that a specific interaction between OPN-i and p85α is essential for sustained expression of Bcl-6 and functional differentiation of both T_{FH} and T_{FR} cells (Supplementary Fig. 8).

Discussion

Signals from the ICOS receptor are essential for Bcl-6 expression and for the initiation and maintenance of T_{FH} and T_{FR} cell differentiation [5, 25, 26]. Here we defined p85α–OPN-i as a molecular link that coupled ICOS engagement to sustained Bcl-6 expression and was essential for differentiation of both T_{FH} and T_{FR} cells. We found that ICOS ligation induced the interaction of the p85α component of PI3K with OPN-i, which promoted OPN-i translocation to the nucleus and protection of Bcl-6 from ubiquitination-dependent degradation. Although early steps of T_{FH} cell differentiation resulting in enhanced *Bcl-6* gene expression and follicular T cell migration depend on cytokines derived from activated DC [30, 31] and may be independent of OPN-i expression, sustained Bcl-6 expression and full T_{FH} and T_{FR} cell differentiation require ICOS-dependent translocation of OPN-i and interaction with Bcl-6. These findings indicate that TCR–ICOS signals known to be essential for sustained differentiation and expansion of T_{FH} and T_{FR} cells preserve Bcl-6 expression in these cells, in contrast to bystander CD4 cells that may undergo early cytokine-dependent activation by DC but fail to activate an ICOS–p85α–OPN-i pathway required for stable Bcl-6 expression.

ICOS activation induces two distinct but overlapping PI3K signaling pathways. The catalytic ICOS–PI3K(p110)–Akt pathway can promote the migration of T_{FH} precursors into B cell follicles [11–13, 32], while we show here that the ICOS–p85α–OPN-i pathway contributed to stable Bcl-6 expression and was essential for sustained follicular T cell responses. The division of labor between the two ICOS-linked PI3K pathways may depend, in part, on distinct environmental cues. MHC-II-independent G-protein coupled signals may facilitate activation of the PI3K(p110)–Akt pathway [12], while engagement of the TCR and

ICOS may promote the PI3K(p85α)–OPN-i pathway and sustained post-transcriptional expression of Bcl-6. TCR–ICOS signals may also indirectly regulate Bcl-6 expression by facilitating Itch-mediated degradation of Foxo1 [33]. Additional studies are needed to define how these pathways are integrated into a functional T_{FH} differentiation program. p85α also functions as a chaperone for the nuclear translocation of the transcription factor XBP-1 after ligation of the insulin receptor [15, 16]. The relatively low intranuclear expression of p85α and its absence from OPN-i–Bcl-6 complexes suggest that p85α may be released before OPN-i engages the intranuclear Bcl-6. The ability of the multi-functional OPN-i adaptor protein to interact with other intranuclear proteins to regulate gene expression by follicular T cells deserves further study [34].

Our findings also indicate that the appropriate balance between T_{FH} and T_{FR} cells is critical for optimal GC responses to infection and avoidance of excessive or autoimmune responses that may result in host tissue destruction. Although T_{FH} and T_{FR} cells share many surface receptors and both require Bcl-6 expression, the molecular elements responsible for their differentiation within the GC follicles have remained unclear. Here we show that the ICOS-dependent induction of OPN-i was required for sustained Bcl-6 expression in both follicular T cell subsets. The magnitude of the GC B cell selection and the associated antibody response depends on cognate T_{FH} cell-antigen-specific B cell interactions. Although OPN deficiency resulted in reduced T_{FR} activity, defective T_{FH} cell responses in the OPN KO mice were not rescued by decreased inhibitory activity of T_{FR} cells. In contrast, selective impairment of OPN-i expression in T_{FR} cells led to substantially increased antibody responses, including the development of high affinity antibodies and autoantibodies, indicating that the OPN-dependent protection of Bcl-6 expression in both follicular $CD4^+$ T cell subsets is essential for control of the germinal center response.

The OPN-i and OPN-s isoforms arise from differential translation of the same mRNA [17]. Although increased expression of *Spp1* gene has been associated with T_{FH}-associated autoimmune disorders and malignancies, the finding that intranuclear OPN contributed to lineage-specific T cell differentiation is unexpected. Mice that overexpress OPN develop a systemic autoimmune disorder [18] that resembles *sanroque* mice with mutations of Roquin (*Rc3h1*), resulting in part from dysregulated ICOS expression [35–37]. Intracellular OPN may promote excessive expression of IFN-α by plasmacytoid dendritic cells (pDC), and contribute to T_H17 cell expansion in the context of SLE [21, 23]. In support of the role of OPN in SLE pathogenesis, expression of OPN in humans with SLE and autoimmune-prone mice (MRL-lpr/lpr) correlates with disease activity [38, 39]. Although high circulating levels of OPN-s may be a useful biomarker for SLE disease activity, separate analysis of OPN-i expression by $CD4^+$ T_{FH} cells and serum OPN may provide a more accurate assessment of SLE status. The finding that disruption of the ICOS–p85α–OPN-i pathway by overexpressing OPN-i mutant inhibited T_{FH} responses and associated autoantibody production also suggests that targeting the p85α–OPN-i interaction may allow inhibition of T_{FH} cell responses and amelioration of systemic autoimmune disease.

Our results also suggest a requirement for continued protection of the Bcl-6 protein from ubiquitination and proteosomal degradation. Bcl-6 represses a group of genes that control lymphocyte differentiation and cell division [4, 40]. Studies of Bcl-6 expression by normal and

neoplastic GC B cells have also suggested that Bcl-6 expression is highly sensitive to post-translational breakdown [4]. Our findings indicate that overexpression of OPN-i leading to enhanced levels of OPN-i–Bcl-6 complexes may result in increased Bcl-6 expression and enhanced T_{FH} cell responses. Indeed, overexpression and nuclear localization of OPN are associated with aggressive T_{FH}-like lymphomas and poor prognosis [41, 42].

We found that OPN-i interacted with the RD2 domain of Bcl-6 to inhibit its ubiquitination-mediated degradation in follicular T cells. A similar interaction between Hsp90 and the Bcl-6 RD2 domain protects Bcl-6 from proteasomal degradation in neoplastic GC B cells [4, 43]. Inhibition of Hsp90 expression or mutation of the BTB domain of Bcl-6 impairs normal and neoplastic GC B cell survival but spares T_{FH} cell differentiation[4, 43–45]. We found that inhibition of OPN-i expression did not affect B cell activity. Excessive Bcl-6 expression may be inhibited by drugs that inhibit post-translational Bcl-6 metabolism [46], including those that target the p85α–OPN-i interaction defined here. Drugs that differentially target the OPN-i–Bcl-6 and Hsp90–Bcl-6 interaction may also allow separate control of follicular T cell and GC B cell responses.

Our findings also bear on efforts to define T_{FH} plasticity and diversity through accurate analysis of Bcl-6 protein by $CD4^+$ T cells. Although expression of Bcl-6 protein returns to basal levels by 2 weeks after immunization, *Bcl-6* mRNA expression remains elevated in "T_{FH}" cells. Precise definition of the T_{FH} response, and its relationship to other T_H subsets, may require coordinate measurements of both Bcl-6 protein and mRNA. In sum, the observations that intranuclear OPN-i protects Bcl-6 from proteasome-associated degradation and allows sustained Bcl-6 expression in T_{FH} cells and T_{FR} cells provides new insight into the ICOS-dependent differentiation of T_{FH} and T_{FR} cells and suggests new therapeutic avenues to manipulate the GC response.

Methods

Mice

C57BL/6J (B6), *Pi3kr1*^{fl}, *Tcr*α$^{-/-}$, *Icos*$^{-/-}$, OT-II transgenic (Jackson Labs), *Rag2*$^{-/-}$*Prf1*$^{-/-}$, B6SJL (CD45.1) (Taconic Farms), B6.Foxp3GFP mice (kindly provided by Dr. H. von Boehmer), *Spp1*$^{\text{flstop}}$ Cre^+ and Cre^- littermates (Supplementary Fig. 2) were housed in pathogen-free conditions and used at 7–12 weeks of age. Deletion of *lox*P-flanked *Pi3kr1* gene in hematopoietic cells was achieved by crossing *Pi3kr1*^{fl} mice with Vav1-Cre (Jackson Labs) that express Cre under the Vav1 promoter. Experiments were performed in an unblinded fashion, with both sexes included for all experiments. For experiments with multiple time points, mice were assigned randomly to each group. All experiments were performed in compliance with federal laws and institutional guidelines as approved by DFCI's Animal Care and Use Committee.

Antibodies and flow cytometry

Fluorescence dye labeled Abs specific for CD4 (L3T4), B220 (RA3-6B2), CD44 (IM7), Fas (15A7), IgM (II/41), T- and B-cell activation antigen (GL7), ICOS (C398.4A), PD-1 (J43), IFNγ (XMG1.2), IL-4 (11B11), IL-17A (eBio17B7), IL-21 (FFA21), Bcl-6 (K112-91) and

FoxP3 (FJK-16s) were purchased from BD, eBioscience and Biolegend. Analysis of CXCR5 expression was performed using a biotinylated anti-CXCR5 (2G8, BD) antibody followed by incubation with APC- or APC.Cy7-labelled streptavidin, as described [25]. Intracellular staining for Bcl-6, FoxP3 and cytokines was performed using the FoxP3 staining buffer set (eBioscience). Intracellular staining of phospho-S473-AKT (M89-61), pSTAT1 (14/P-STAT1), pSTAT3 (4/P-STAT3) was conducted according to manufacturer's instructions (BD Bioscience). Cells were acquired on a FACSCantoII using FACSDIva software (BD Biosciences) and analyzed with FlowJo software (Tristar).

Adoptive transfer and immunization

FACS-sorted $CD4^+$ T cell subsets and B cells purified using B lymphocyte enrichment set (BD Bioscience) were transferred into indicated hosts before immunization with protein antigens emulsified in CFA. In some experiments, reimmunization with protein antigens in IFA at the indicated times was performed. All immunizations were conducted by intraperitoneal injection. Serum was prepared at the indicated time for measurement of primary and secondary antibody titers.

Enzyme-linked immunosorbent assay (ELISA)

Detection of NP-specific antibodies was performed as described [47]. Analysis of anti-mouse collagen antibody was performed as described [48]. Determination of pAkt and Akt levels was conducted using InstantOne™ ELISA kit (eBioscience).

In vitro differentiation of T_H subsets

OT-II $CD25^-CD4^+$ T cells (2×10^5 cells/ml) purified from the indicated mouse strains using CD4 T lymphocyte enrichment set (BD Bioscience) were stimulated with 1 μg/ml OT-II peptide (ISQAVHAAHAEINEAGR) in the presence of irradiated total splenocytes (2×10^6 cells/ml). The cytokine and antibody mixtures used for differentiation of CD4 cells to each T_H cell subset were described previously [49]. Cytokine production after incubation ×5 d was analyzed by ELISA, according to manufacturer's instructions (RD systems).

Plasmids and generation of retrovirus

OPN-i expression vectors, pMLS5, OPN-i–Flag, and OPN-i–GFP were described previously [17]. A tandem HA-Flag tag was introduced at the C-terminus of OPN-i cDNA by PCR using primers containing *BamHI* and *EcoRI* sites followed by cloning into pBABE-GFP vector. Bcl-6 cDNA was obtained from Open Biosystems (Bcl-6 Clone ID: 6309948), sequenced in full, before complete coding region sequences were cloned inframe with a Flag tag at the N-terminus into retroviral expression vector MSCV-IRES-GFP. The following plasmids were obtained from Addgene: p85α (plasmid 1399 and 1407), HA-p110 (plasmid 12522 and 15691) [50, 51] and HA-Ub (plasmid 17608) [52]. Deletion constructs of Bcl-6, Flag–Bcl-6, and OPN-i Y166F mutants were generated by PCR-mediated mutagenesis with the QuickChange II XL Site-Directed Mutagenesis Kit (Agilent). The accuracy of all plasmids was confirmed by DNA sequencing. Retroviral stocks were generated by transfection of 293T cells with plasmids expressing pBABE-GFP control or pBABE-GFP plus OPN-i wild-type or OPN-i Y166F along with pCL-Eco packaging vector using TransIT-LT1 transfection

reagent (Mirus). Viral supernatants were collected 72 h later before infection of $CD4^+$ T cells, as described below.

Retroviral transduction

Purified naive $CD4^+$ T cells from the indicated mouse strains were stimulated with plate-bound anti-CD3 (5 μg/ml) and anti-CD28 (5 μg/ml) in the presence of 10 ng/ml human IL-2 (hIL-2). 24–36 h post-stimulation, $CD4^+$ T cells were infected with retrovirus expressing GFP and the indicated protein in the presence of 8 μg/ml of polybrene before 1 h centrifugation at 2000 rpm followed by 6–8 h at 37°C and subsequent replacement of three quarters of hIL2-containing fresh medium. After 3 d of stimulation, $CD4^+$ T cells were rested in the presence of hIL-2 for 1–2 d before sorting for GFP^+CD4^+ T cells followed by adoptive transfer into *Rag2*$^{-/-}$*Prf1*$^{-/-}$ hosts and resting *in vivo* for 2 d prior to immunization as described above. In Fig. 8c, *Rag2*$^{-/-}$*Prf1*$^{-/-}$ hosts were transferred with sorted GFP^+ CII-immune $CD4^+$ T cells and purified B cells followed by immunization with chicken CII in CFA and boosting with CII in IFA, as described previously [48]. Retroviral infection of $CD25^+CD4^+$ T cells was adapted from Haxhinasto *et al* [27]. Briefly, purified $CD25^+CD4^+$ T cells were stimulated with plate-bound anti-CD3 (5 μg/ml) and anti-CD28 (5 μg/ml) in the presence of 1,000 U/ml hIL-2 and 20 ng/ml TGFβ. Three days post-stimulation, cells were infected with retrovirus expressing GFP and the indicated protein, as described above, for a total of 2 d before sorting GFP^+ cells and transfer.

Immunoprecipitation and Immunoblot

The procedure was performed as described previously [21]. The following antibodies were used: p85α (Z-8) and Bcl-6 (N-3 or C-19) (Santa Cruz); Flag (M2) and actin (AC-15) (Sigma); Lamin B1 (L-5) (Invitrogen); OPN (O-17) (IBL American); tubulin (AA2) (Millipore) and HA (C29F4) (Cellsignal). Band intensity was quantified using ImageJ software, version 1.45b (NIH).

Immunofluorescence staining

$CD62L^-CD4^+$ T cells (> 95%) from the indicated mouse strains injected with KLH in CFA were purified with MACS $CD4^+CD62L^+$ T-cell isolation kit (Miltenyi) and stimulated with anti-ICOS for the indicated times before fixation, permeabilization and immunostaining. Antibodies or dyes used include: rabbit Bcl-6 (N-3), anti-rabbit Alexa Fluor 568 (for Bcl-6); mouse OPN (AKm2A1, Santa Cruz), anti-mouse Alexa Fluor 647 (for OPN) and nuclear dye DAPI. Images were captured through a 63× objective lens with a Leica SP5X laser scanning confocal microscope and analyzed using ImageJ software, version 1.45b (NIH).

Gene expression profiling

Naïve $CD4^+$ T cells (> 95%) were purified from single cell suspensions of B6 spleen using the MACS $CD4^+CD62L^+$ T-cell isolation kit (Miltenyi) and stimulated with anti-CD3 (5 μg/ml) and anti-CD28 (2 μg/ml) for 2 d followed by resting overnight before 20 min of incubation with anti-CD3 (0.2 μg/ml) and/or anti-ICOS (5 μg/ml) and cross-linking with goat anti-hamster Ab (20 μg/ml) for 8 h. RNA was prepared with the RNeasy plus micro kit according to the manufacturer's instructions (Qiagen). RNA amplification, labeling and

hybridization to Mouse Gene 1.0 ST Array (Affymetrix) were performed at the Microarray Core Facility (Dana Farber Cancer Institute), with quadruplicates for anti-CD3 ligation alone and duplicates for anti-CD3 and anti-ICOS co-stimulation. Data were deposited in the GEO database under accession number GSE61284.

Quantitative RT-PCR

RNA was extracted using RNeasy plus micro kit (Qiagen) before quantitative real time PCR was performed with TaqMan gene expression assays [*Spp1* (Mm00436767_m1), *Bcl-6* (Mm00477633_m1), *Prdm1* (Mm00476128_m1), *Rps18* (Mm02601777_g1)] and RNA-to-CT™ *1-Step* Kit (Life Technologies). All results were first normalized to those of the *Rps18* control and are presented as normalized expression for the sample relative to the appropriate comparison conditions, as indicated in the legends.

Statistical analyses

Statistical analyses were performed using two-tailed, unpaired Student's t-test or Mann-Whitney test with the assumption of equal sample variance, with GraphPad Prism V6 software. Error bars indicate mean ± s.e.m. A P value <0.05 was considered to be statistically significant (* = <0.05, ** = <0.01, *** = <0.001). No exclusion of data points was used. Sample size was not specifically predetermined, but the number of mice used was consistent with previous experience with similar experiments.

Supplementary Material

Refer to Web version on PubMed Central for supplementary material.

Acknowledgments

We thank Kai Wucherpfennig for critical reading and Lewis Cantley, Ted Dawson, Shinya Yamanaka and Jean Zhao for provision of plasmids. We thank Dr. Lisa Cameron (DFCI Microscopy Core) for help with image preparation and analysis, Yue Shao (DFCI Microarray Facility) for microarray analysis, and A. Angel for manuscript and figure preparation. This work was supported in part by NIH Research Grant AI48125 and a gift from The LeRoy Schecter Research Foundation to HC; the Benacerraf Fellowship and NRSA Fellowship (T32 CA070083) to JWL; and a Belgian-American Educational Foundation Fellowship to BV.

Literature cited

1. Johnston RJ, et al. Bcl6 and Blimp-1 are reciprocal and antagonistic regulators of T follicular helper cell differentiation. Science. 2009; 325:1006–1010. [PubMed: 19608860]
2. Nurieva RI, et al. Bcl6 mediates the development of T follicular helper cells. Science. 2009; 325:1001–1005. [PubMed: 19628815]
3. Yu D, et al. The transcriptional repressor Bcl-6 directs T follicular helper cell lineage commitment. Immunity. 2009; 31:457–468. [PubMed: 19631565]
4. Bunting KL, Melnick AM. New effector functions and regulatory mechanisms of BCL6 in normal and malignant lymphocytes. Curr Opin Immunol. 2013; 25:339–346. [PubMed: 23725655]
5. Sage PT, Francisco LM, Carman CV, Sharpe AH. The receptor PD-1 controls follicular regulatory T cells in the lymph nodes and blood. Nat Immunol. 2013; 14:152–161. [PubMed: 23242415]
6. Linterman MA, et al. Foxp3(+) follicular regulatory T cells control the germinal center response. Nat Med. 2011; 17:975–982. [PubMed: 21785433]
7. Chung Y, et al. Follicular regulatory T cells expressing Foxp3 and Bcl-6 suppress germinal center reactions. Nat Med. 2011; 17:983–988. [PubMed: 21785430]

8. Crotty S. Follicular helper CD4 T cells (TFH). Annual Reviews of Immunology. 2011; 29:621–663.
9. Baumjohann D, Okada T, Ansel KM. Cutting Edge: Distinct waves of BCL6 expression during T follicular helper cell development. J Immunol. 2011; 187:2089–2092. [PubMed: 21804014]
10. Gigoux M, et al. Inducible costimulator promotes helper T-cell differentiation through phosphoinositide 3-kinase. Proc Natl Acad Sci U S A. 2009; 106:20371–20376. [PubMed: 19915142]
11. Xu H, et al. Follicular T-helper cell recruitment governed by bystander B cells and ICOS-driven motility. Nature. 2013; 496:523–527. [PubMed: 23619696]
12. Kang SG, et al. MicroRNAs of the miR-17 approximately 92 family are critical regulators of TFH differentiation. Nat Immunol. 2013; 14:849–857. [PubMed: 23812097]
13. Rolf J, Fairfax K, Turner M. Signaling pathways in T follicular helper cells. Journal of Immunology. 2010; 184:6563–6568.
14. Yu J, et al. Regulation of the p85/p110 phosphatidylinositol 3′-kinase: stabilization and inhibition of the p110alpha catalytic subunit by the p85 regulatory subunit. Mol Cell Biol. 1998; 18:1379–1387. [PubMed: 9488453]
15. Park SW, et al. The regulatory subunits of PI3K, p85alpha and p85beta, interact with XBP-1 and increase its nuclear translocation. Nat Med. 2010; 16:429–437. [PubMed: 20348926]
16. Winnay JN, Boucher J, Mori MA, Ueki K, Kahn CR. A regulatory subunit of phosphoinositide 3-kinase increases the nuclear accumulation of X-box-binding protein-1 to modulate the unfolded protein response. Nat Med. 2010; 16:438–445. [PubMed: 20348923]
17. Shinohara ML, Kim HJ, Kim JH, Garcia VA, Cantor H. Alternative translation of Osteopontin generates intracellular and secreted isoforms that mediate distinct biological activities in dendritic cells. Proc Natl Acad Sci USA. 2008; 105:7235–7239. [PubMed: 18480255]
18. Cantor H, Shinohara ML. Regulation of T-helper-cell lineage development by osteopontin: the inside story. Nat Rev Immunol. 2009; 9:137–141. [PubMed: 19096390]
19. Ashkar S, et al. Eta-1 (osteopontin): an early component of Type 1(cell-mediated) immunity. Science. 2000; 287:860–864. [PubMed: 10657301]
20. Shinohara ML, et al. T-bet-dependent expression of osteopontin contributes to T cell polarization. Proc Natl Acad Sci U S A. 2005; 102:17101–17106. [PubMed: 16286640]
21. Shinohara ML, et al. Osteopontin expression is essential for IFN-à production by plasmacytoid dendritic cells. Nat Immunol. 2006; 7:498–506. [PubMed: 16604075]
22. Patarca R, Wei FY, Iregui MV, Cantor H. Differential induction of interferon-gamma gene expression after activation of CD4+ T-cells by conventional antigen and Mls superantigen. Proceedings of the National Academy of Science USA. 1991; 88:2736–2739.
23. Shinohara ML, Kim JH, Garcia VA, Cantor H. Engagement of the Type-I interferon receptor on dendritic cells inhibits promotion of Th17 cells: Role of intracellular Osteopontin. Immunity. 2008; 29:68–78. [PubMed: 18619869]
24. Kerfoot SM, et al. Germinal center B cell and T follicular helper cell development initiates in the interfollicular zone. Immunity. 2011; 34:947–960. [PubMed: 21636295]
25. Choi YS, et al. ICOS receptor instructs T follicular helper cell versus effector cell differentiation via induction of the transcriptional repressor Bcl6. Immunity. 2011; 34:932–946. [PubMed: 21636296]
26. Chang JH, et al. TRAF3 regulates the effector function of regulatory T cells and humoral immune responses. J Exp Med. 2014; 211:137–151. [PubMed: 24378539]
27. Haxhinasto S, Mathis D, Benoist C. The AKT-mTOR axis regulates de novo differentiation of CD4+Foxp3+ cells. J Exp Med. 2008; 205:565–574. [PubMed: 18283119]
28. Obenauer JC, Cantley LC, Yaffe MB. Scansite 2.0: Proteome-wide prediction of cell signaling interactions using short sequence motifs. Nucleic Acids Res. 2003; 31:3635–3641. [PubMed: 12824383]
29. Yaffe MB, et al. A motif-based profile scanning approach for genome-wide prediction of signaling pathways. Nat Biotechnol. 2001; 19:348–353. [PubMed: 11283593]

30. Choi YS, Eto D, Yang JA, Lao C, Crotty S. Cutting edge: STAT1 is required for IL-6-mediated Bcl6 induction for early follicular helper cell differentiation. J Immunol. 2013; 190:3049–3053. [PubMed: 23447690]
31. Nakayamada S, et al. Type I IFN Induces Binding of STAT1 to Bcl6: Divergent Roles of STAT Family Transcription Factors in the T Follicular Helper Cell Genetic Program. J Immunol. 2014
32. Rolf J, et al. Phosphoinositide 3-kinase activity in T cells regulates the magnitude of the germinal center reaction. J Immunol. 2010; 185:4042–4052. [PubMed: 20826752]
33. Xiao N, et al. The E3 ubiquitin ligase Itch is required for the differentiation of follicular helper T cells. Nat Immunol. 2014; 15:657–666. [PubMed: 24859451]
34. Inoue M, Shinohara ML. Intracellular osteopontin (iOPN) and immunity. Immunologic research. 2011; 49:160–172. [PubMed: 21136203]
35. Vinuesa CG, et al. A RING-type ubiquitin ligase family member required to repress follicular helper T cells and autoimmunity. Nature. 2005; 435:452–458. [PubMed: 15917799]
36. Yu D, et al. Roquin represses autoimmunity by limiting inducible T-cell co-stimulator messenger RNA. Nature. 2007; 450:299–303. [PubMed: 18172933]
37. Glasmacher E, et al. Roquin binds inducible costimulator mRNA and effectors of mRNA decay to induce microRNA-independent post-transcriptional repression. Nat Immunol. 2010; 11:725–733. [PubMed: 20639877]
38. Patarca R, Wei FY, Singh P, Morasso MI, Cantor H. Dysregulated expression of the T-cell cytokine Eta-1 in CD4-8- lymphocytes during the development of murine autoimmune disease. Journal of Experimental Medicine. 1990; 172:1177–1183. [PubMed: 1976736]
39. Wong CK, Lit LC, Tam LS, Li EK, Lam CW. Elevation of plasma osteopontin concentration is correlated with disease activity in patients with systemic lupus erythematosus. Rheumatology (Oxford). 2005; 44:602–606. [PubMed: 15705633]
40. Crotty S, Johnston RJ, Schoenberger SP. Effectors and memories: Bcl-6 and Blimp-1 in T and B lymphocyte differentiation. Nat Immunol. 2010; 11:114–120. [PubMed: 20084069]
41. Powell JA, et al. Expression profiling of a hemopoietic cell survival transcriptome implicates osteopontin as a functional prognostic factor in AML. Blood. 2009; 114:4859–4870. [PubMed: 19805619]
42. Tun HW, et al. Pathway analysis of primary central nervous system lymphoma. Blood. 2008; 111:3200–3210. [PubMed: 18184868]
43. Cerchietti LC, et al. A purine scaffold Hsp90 inhibitor destabilizes BCL-6 and has specific antitumor activity in BCL-6-dependent B cell lymphomas. Nat Med. 2009; 15:1369–1376. [PubMed: 19966776]
44. Huang C, Hatzi K, Melnick A. Lineage-specific functions of Bcl-6 in immunity and inflammation are mediated by distinct biochemical mechanisms. Nat Immunol. 2013; 14:380–388. [PubMed: 23455674]
45. Polo JM, et al. Specific peptide interference reveals BCL6 transcriptional and oncogenic mechanisms in B-cell lymphoma cells. Nat Med. 2004; 10:1329–1335. [PubMed: 15531890]
46. Kronke J, et al. Lenalidomide causes selective degradation of IKZF1 and IKZF3 in multiple myeloma cells. Science. 2014; 343:301–305. [PubMed: 24292625]
47. Kim HJ, Verbinnen B, Tang X, Lu L, Cantor H. Inhibition of follicular T helper cells by CD8 + Treg is essential for self tolerance. Nature. 2010; 467:328–332. [PubMed: 20844537]
48. Leavenworth JW, Tang X, Kim HJ, Wang X, Cantor H. Amelioration of arthritis through mobilization of peptide-specific $CD8^+$ regulatory T cells. Journal of Clinical Investigation. 2013; 123:1382–1389. [PubMed: 23376792]
49. Leavenworth JW, Wang X, Wenander CS, Spee P, Cantor H. Mobilization of natural killer cells inhibits development of collagen-induced arthritis. Proc Natl Acad Sci USA. 2011; 108:14584–14589. [PubMed: 21873193]
50. Takahashi K, Mitsui K, Yamanaka S. Role of ERas in promoting tumour-like properties in mouse embryonic stem cells. Nature. 2003; 423:541–545. [PubMed: 12774123]
51. Zhao JJ, et al. The oncogenic properties of mutant p110alpha and p110beta phosphatidylinositol 3-kinases in human mammary epithelial cells. Proc Natl Acad Sci U S A. 2005; 102:18443–18448. [PubMed: 16339315]

52. Lim KL, et al. Parkin mediates nonclassical, proteasomal-independent ubiquitination of synphilin-1: implications for Lewy body formation. The Journal of neuroscience: the official journal of the Society for Neuroscience. 2005; 25:2002–2009. [PubMed: 15728840]

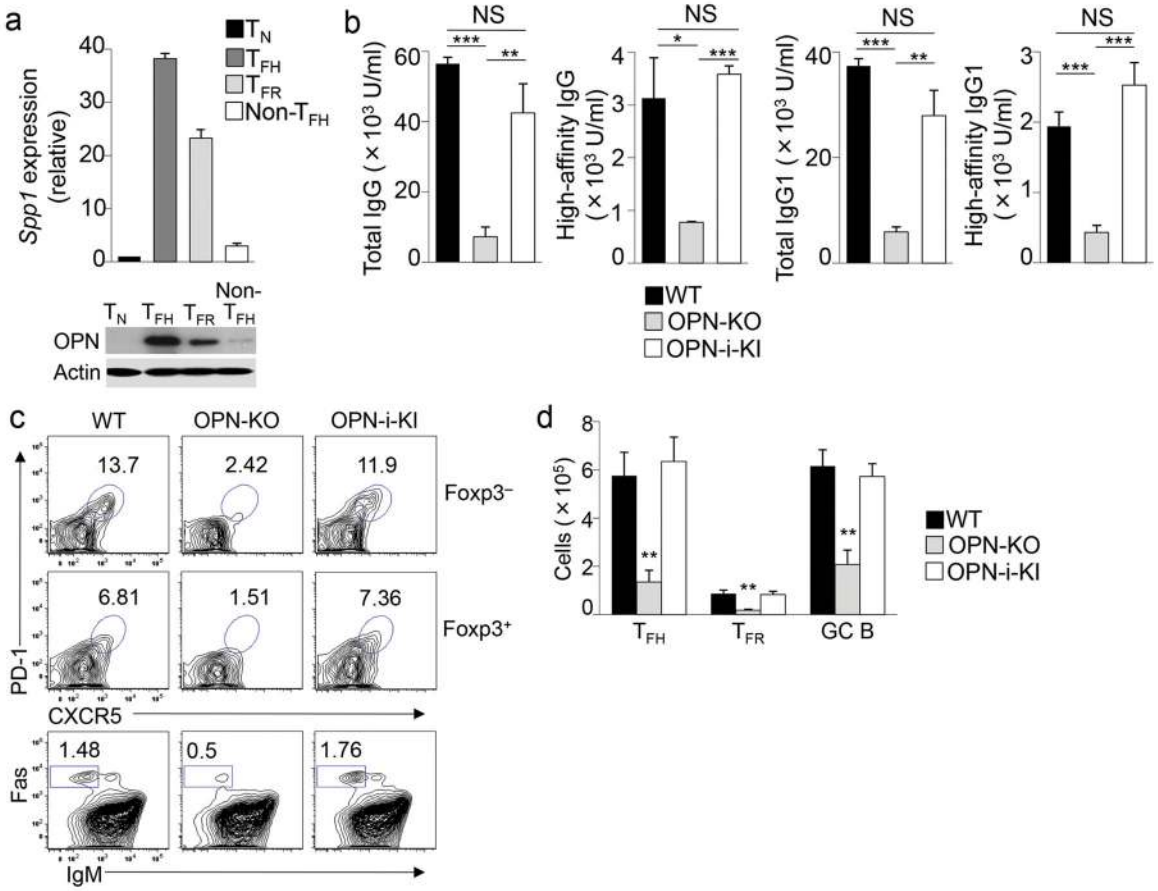

Figure 1.

OPN regulates T_{FH} and T_{FR} cell differentiation.

a, Quantitative RT-PCR analysis of *Spp1* mRNA (top) and immunoblot analysis of OPN and actin protein levels (bottom) expressed by $CD4^+$ T cell subsets sorted (as shown in Supplementary Fig. 1) from pooled B6 mice ($n = 16$) 3 d after injection with KLH in CFA. *Spp1* expression was normalized to the *Rps18* control and results are presented relative to naïve T cells (T_N), set as 1. **b,** Titers of total (NP_{23}) and high-affinity (NP_4) NP-specific IgG and IgG1 in serum of OT-II, OT-II OPN-KO and OT-II OPN-i-KI mice that were immunized i.p. with NP_{13}-OVA in CFA, challenged with NP_{13}-OVA in IFA 10 d later, and analyzed 7 d post-challenge. **c,** Flow cytometry of splenocytes from mice in **b.** Numbers indicate percent T_{FH} ($Foxp3^-PD1^+CXCR5^+CD4^+$), T_{FR} ($Foxp3^+PD1^+CXCR5^+CD4^+$) and GC B ($Fas^+IgM^-B220^+$) cells. **d,** Numbers of T_{FH}, T_{FR} and GC B cells in **c** ($n = 6$ per group). $^*P < 0.05$, $^{**}P < 0.01$ and $^{***}P < 0.001$ (unpaired two-tailed Student's t-test); NS, not significant. Data are representative of two (**a**) and at least three independent experiments (**b–d**) (error bars, mean ± s.e.m).

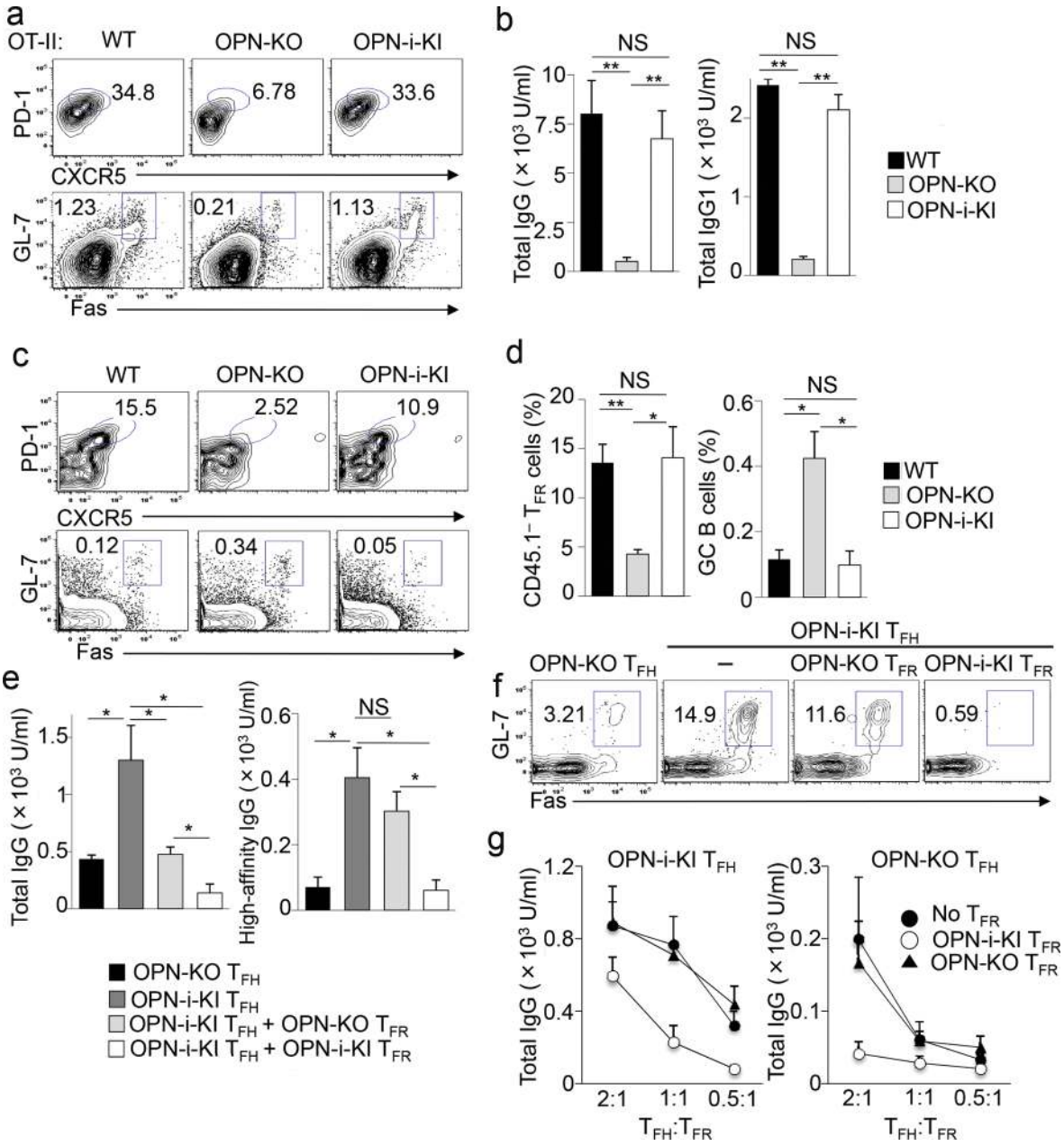

Figure 2.

The OPN-i deficient T_{FH} and T_{FR} phenotype is cell-intrinsic.

a, Flow cytometry of donor OT-II $CD4^+$ T cells from spleens of *Rag2*$^{-/-}$*Prf1*$^{-/-}$ hosts transferred with naïve OT-II, OT-II OPN-KO and OT-II OPN-i-KI $CD4^+$ T cells along with wild-type B cells, followed by immunization with NP_{13}-OVA in CFA and analysis 10 d later. Numbers indicate percent T_{FH} ($Foxp3^-PD1^+CXCR5^+CD4^+$) and GC B ($Fas^+GL7^+B220^+$) cells. **b,** Serum titers of total (NP_{23}) NP-specific IgG and IgG1 from recipient mice in **a** ($n = 6$ per group). **c,** Flow cytometry of donor Treg from spleens of *Tcra*$^{-/-}$ hosts transferred with sorted $CD45.2^+$ Treg ($CD25^{hi}CD44^{int}CXCR5^-CD4^+$) from the indicated mice and $CD45.1^+$ wild-type naïve $CD4^+$ T cells

($CD25^{-}GITR^{-}CD44^{lo}CD62L^{hi}$) at a ratio of 1:2, followed by immunization with NP_{26}-KLH in CFA and analysis 10 d later. Numbers indicate percent T_{FR} ($CD45.1^{-}CD44^{+}Foxp3^{+}PD1^{+}CXCR5^{+}CD4^{+}$) and GC B ($Fas^{+}GL7^{+}B220^{+}$) cells. **d,** Frequency of T_{FR} and GC B cells in **c** ($n = 5$ per group). **e,** Titers of total (NP_{23}) and high-affinity (NP_4) NP-specific IgG at d14 in immunized $Rag2^{-/-}Prf1^{-/-}$ recipients of OPN-i-KI or OPN-KO T_{FH} cells (5×10^4) and/or OPN-i-KI or OPN-KO T_{FR} cells (2.5×10^4) (sorted as in Supplementary Fig. 1) and wild-type GL-7^{-} B cells (1×10^5) from KLH-immunized mice. All recipients ($n = 4$ per group) were immunized with NP_{26}-KLH in CFA. **f,** Donor GC B cells from spleens of recipients in **e** (in same order from left to right) at d22. **g,** Titers of NP-specific total IgG at d11 in immunized $Rag2^{-/-}Prf1^{-/-}$ mice ($n = 3$ per transfer) given OPN-i-KI or OPN-KO T_{FH} cells and/or OPN-i-KI or OPN KO T_{FR} cells (2.5×10^4) at different ratios and wild-type GL-7^{-} B cells (1×10^5) from KLH-immunized mice. Data are representative of three (**a–b**) and two (**c–g**) independent experiments. $^{*}P < 0.05$ and $^{**}P < 0.01$ (unpaired two-tailed Student's t-test; error bars, mean ± s.e.m).

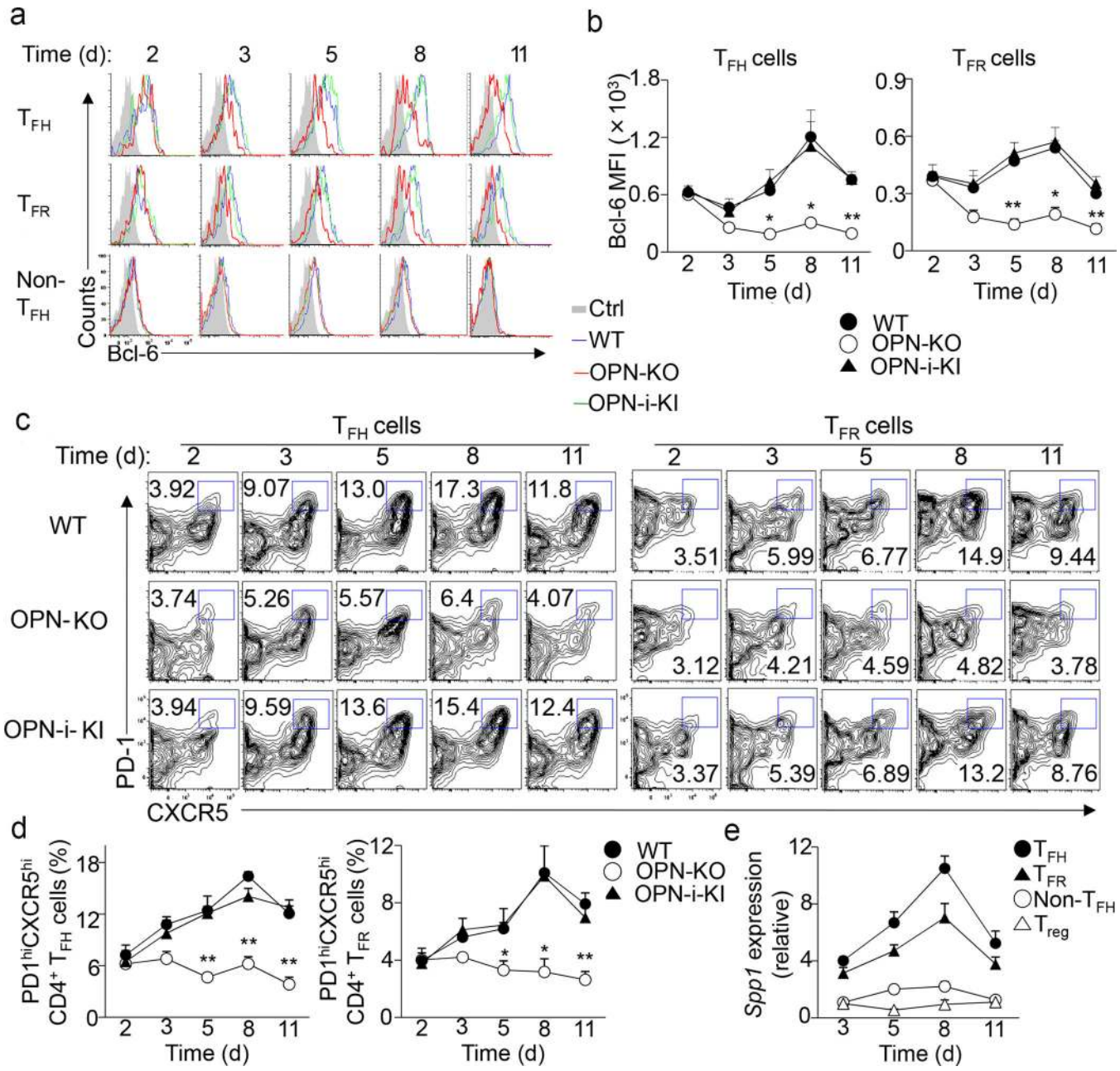

Figure 3.

OPN-i deficiency impairs Bcl-6 protein expression.

a–b, Flow cytometry of splenocytes from the indicated mice at day 2–11 after immunization with KLH in CFA. Overlay of histograms of intracellular Bcl-6 expression in $CD4^+$ T_H subsets (as defined in Supplementary Fig. 1) (**a**) and quantitation of Bcl-6 MFI (**b**). **c,** T_{FH} ($CD4^+CD44^{hi}CXCR5^+PD\text{-}1^+Foxp3^-$) and T_{FR} ($CD4^+CD44^{hi}CXCR5^+PD\text{-}1^+Foxp3^+$) cell differentiation from mice in **a**. Numbers indicate percent $PD1^+CXCR5^+$ cells. **d,** Frequency of T_{FH} and T_{FR} cells in **c** (n = 3–4 per time point per group). **e,** Quantitative RT-PCR analysis of *Spp1* mRNA in $CD4^+$ T cell subsets sorted (as in Supplementary Fig. 1) from pooled OPN-i-KI mice (n = 3–7 per time point) at day 3–11 after immunization with KLH in

CFA. *Spp1* expression was normalized to the *Rps18* control and results are presented relative to that of T_{reg} at day 3, set as 1. Data represent two (**a–e**) independent experiments. $*P < 0.05$ and $**P < 0.01$ (unpaired two-tailed Student's t-test; error bars, mean ± s.e.m or s.d. in **e**).

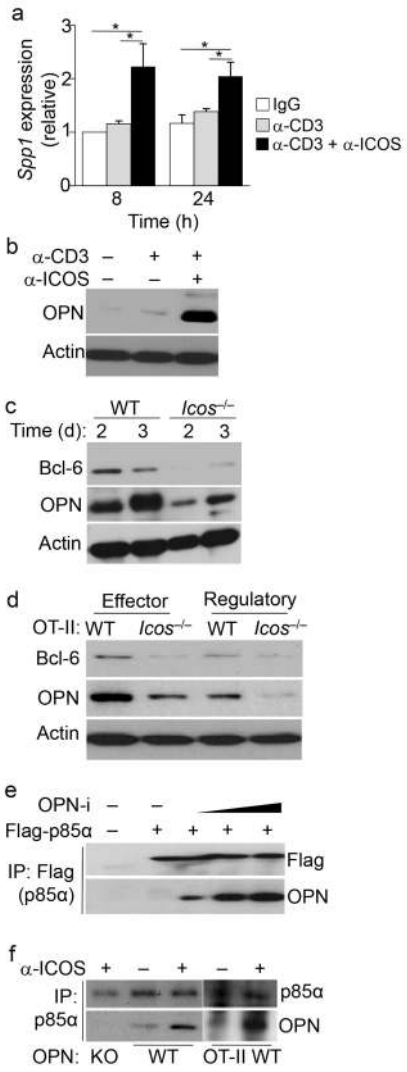

Figure 4.

ICOS co-stimulation promotes an interaction between OPN-i and p85α.

a, Quantitative RT-PCR analysis of *Spp1* mRNA in naïve $CD4^+$ T cells from B6 mice stimulated with anti-CD3 and anti-CD28 for 2 d, followed by resting overnight before 20 m incubation with the indicated Abs and cross-linking with goat anti-hamster Ab for 8 h or 24 h. *Spp1* expression was normalized to the *Rps18* control and results are presented relative to isotype-matched hamster IgG-treated cells at 8 h, set as 1. $*P < 0.05$ (unpaired two-tailed Student's t-test; error bars, mean ± s.e.m of quadruplicates). **b,** Immunoblot analysis of OPN and actin of $CD4^+$ T cells in **a** after 12 h cross-linking. **c,** Immunoassay of lysates of purified $CD62L^-$ $CD4^+$ T cells from $Icos^{-/-}$ and wild-type mice 2 or 3 d after intraperitoneal injection with 100 μg KLH in CFA, probed with anti-Bcl-6, anti-OPN and anti-actin. **d,** Immunoblot analysis of lysates of sorted $V_\beta5^+CD25^-CD44^{hi}GITR^-CD4^+$ effector and $CD25^+CD44^{hi}GITR^+CD4^+$ regulatory T cells from pooled OT-II ($n = 10$) or OT-II $Icos^{-/-}$ mice ($n = 15$) 8 d post-immunization with OVA in CFA, probed as in **c. e,** Immunoassay of lysates of 293T cells transfected with plasmids encoding Flag-tagged p85α (Flag-p85α) and

increasing concentrations of OPN-i, assessed by immunoprecipitation (IP) with anti-Flag and immunoblot analysis with anti-Flag and anti-OPN. **f,** Immunoassay of lysates of purified naïve $CD4^+$ T cells from OPN-KO and wild-type mice stimulated with anti-CD3 and anti-CD28 for 2 d (left); or $CD44^+CD4^+$ T cells from OT-II mice 4 d post-immunization with OVA in CFA (right), followed by resting and re-stimulation with anti-CD3 and/or anti-ICOS (as in **a**) for 12 h, and assessed by IP with anti-p85α and immunoblot analysis with anti-p85α and anti-OPN. Data represent two (**a, c, d**) and three (**b, e, f**) independent experiments.

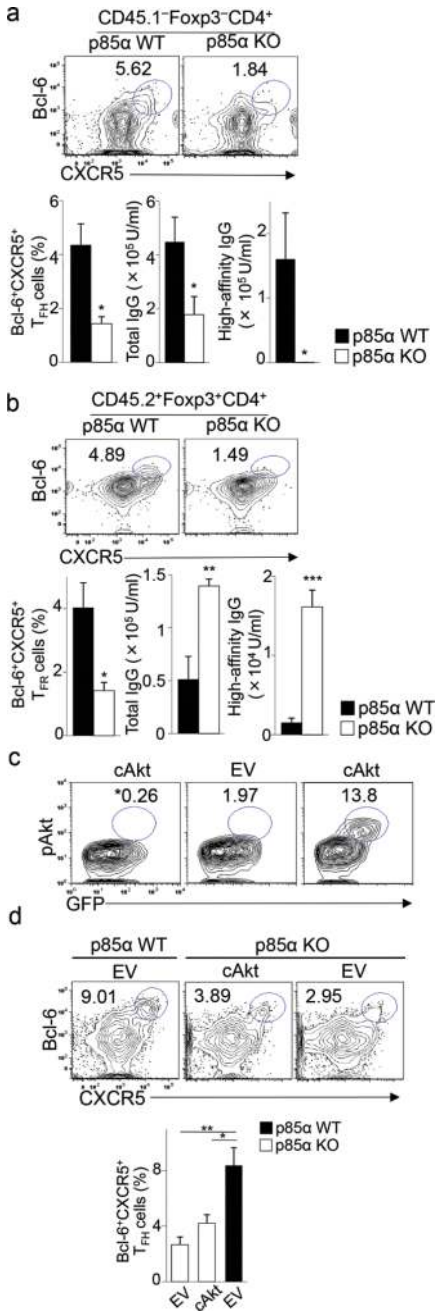

Figure 5.

p85α is required for T_{FH} and T_{FR} cell differentiation.

a, Flow cytometry of donor CD4$^+$ T cells from spleens of *Rag2*$^{-/-}$*Prf1*$^{-/-}$ hosts transferred with p85α WT or p85α KO naïve CD4$^+$ T cells along with CD45.1$^+$ wild-type B cells, followed by immunization with NP_{26}-KLH in CFA and analysis 10 d later. Numbers indicate percent CD45.1$^-$Foxp3$^-$Bcl-6$^+$CXCR5$^+$ T_{FH} cells. Bottom panel, frequency of T_{FH} cells and titers of NP-specific total (NP_{23}) and high-affinity (NP_4) IgG in immunized recipients (n = 3–4 per group). **b,** Flow cytometry of donor CD4$^+$ Treg from spleens of *Tcra*$^{-/-}$ hosts transferred with CD45.2$^+$ p85α WT or p85α KO CD4$^+$ Treg along with

CD45.1$^+$ naïve CD4$^+$ T cells, followed by immunization with NP_{26}-KLH in CFA and analysis 10 d later. Numbers indicate percent CD45.2$^+$Foxp3$^+$Bcl-6$^+$CXCR5$^+$ T_{FR} cells. Bottom panel, frequency of T_{FR} cells and titers of NP-specific total (NP_{23}) and high-affinity (NP_4) IgG in immunized recipients (n = 3–6 per group). **c**, Flow cytometry of p85α KO CD4$^+$ T cells transduced with retroviral vector expressing GFP alone (empty vector [EV]) or GFP and constitutively-active Akt (cAkt). Numbers indicate percent GFP$^+$pAkt$^+$ (phospho-Akt) cells. *, isotype control for pAkt staining. **d,** (top panel) Flow cytometry of donor CD4$^+$ T cells from spleens of *Rag2*$^{-/-}$*Prf1*$^{-/-}$ hosts transferred with p85α KO or p85α WT CD4$^+$ T cells transduced with retroviral vectors (as described in **c**) along with wild-type B cells, followed by immunization with NP_{26}-KLH in CFA and analysis 5 d post-immunization. Numbers indicate percent Bcl-6$^+$CXCR5$^+$ cells. Bottom panel, frequency of Bcl-6$^+$CXCR5$^+$CD4$^+$ T cells (n = 4 per group). Data are representative of two (**a–d**) independent experiments. *P < 0.05, **P < 0.01 and ***P < 0.001 (unpaired two-tailed Student's t-test; error bars, mean ± s.e.m).

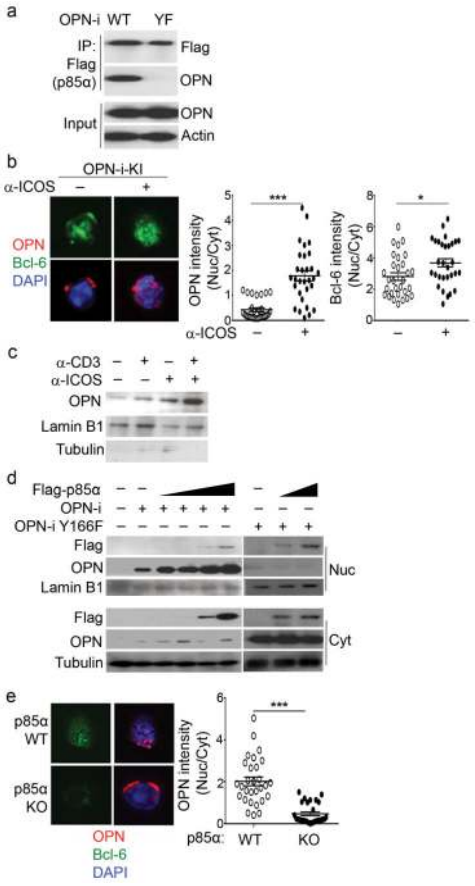

Figure 6.

p85α chaperones nuclear translocation of OPN-i.

a, Immunoassay of lysates of 293T cells transfected with plasmids encoding Flag-p85α and OPN-i wild-type or OPN-i Y166F (YF) mutant, assessed by immunoprecipitation with anti-Flag and immunoblot analysis with anti-Flag and anti-OPN. Input, immunoblot analysis of an aliquot of cell lysates without IP. **b,** Confocal microscopy of OPN and Bcl-6 expression by $CD44^{+}CD4^{+}$ T cells from OPN-i-KI mice 3 d post-injection with KLH in CFA, followed by cross-linking with anti-ICOS Ab (as in Fig. 4a) *in vitro*. Cells were counterstained with DNA-intercalating dye DAPI to trace nuclear perimeters. About 25–30 cells stained with Bcl-6 were further analyzed for localization of OPN protein. Right, fluorescence intensity expressed as the mean ratio of nuclear (Nuc) to cytoplasmic (Cyt) fluorescence pixel intensity (n = 25–30 cells). **c,** Immunoblot analysis of nuclear fractions of OPN-i-KI $CD62L^{-}CD4^{+}$ T cells treated with anti-CD3 and/or anti-ICOS Abs (as in Fig. 4a), probed with anti-OPN, anti-Lamin B1 and anti-tubulin (to validate the integrity of nuclear separation). **d**, Immunoblot analysis of nuclear and cytosolic fractions of 293T cells transfected with plasmids encoding OPN-i wild-type or OPN-i Y166F mutant and increasing concentrations of Flag-p85α, probed with Abs, as indicated. **e,** Confocal microscopy of OPN and Bcl-6 expression by $CD62L^{-}$ $CD4^{+}$ T cells from p85α WT or KO mice. Cell treatment and analysis as in **a**. Original magnification (**b, e**), 600×. $*P < 0.05$ and $***P < 0.001$, Mann-Whitney test (error bars, mean ± s.e.m) **(b, e)**. All results are representative of at least two independent experiments.

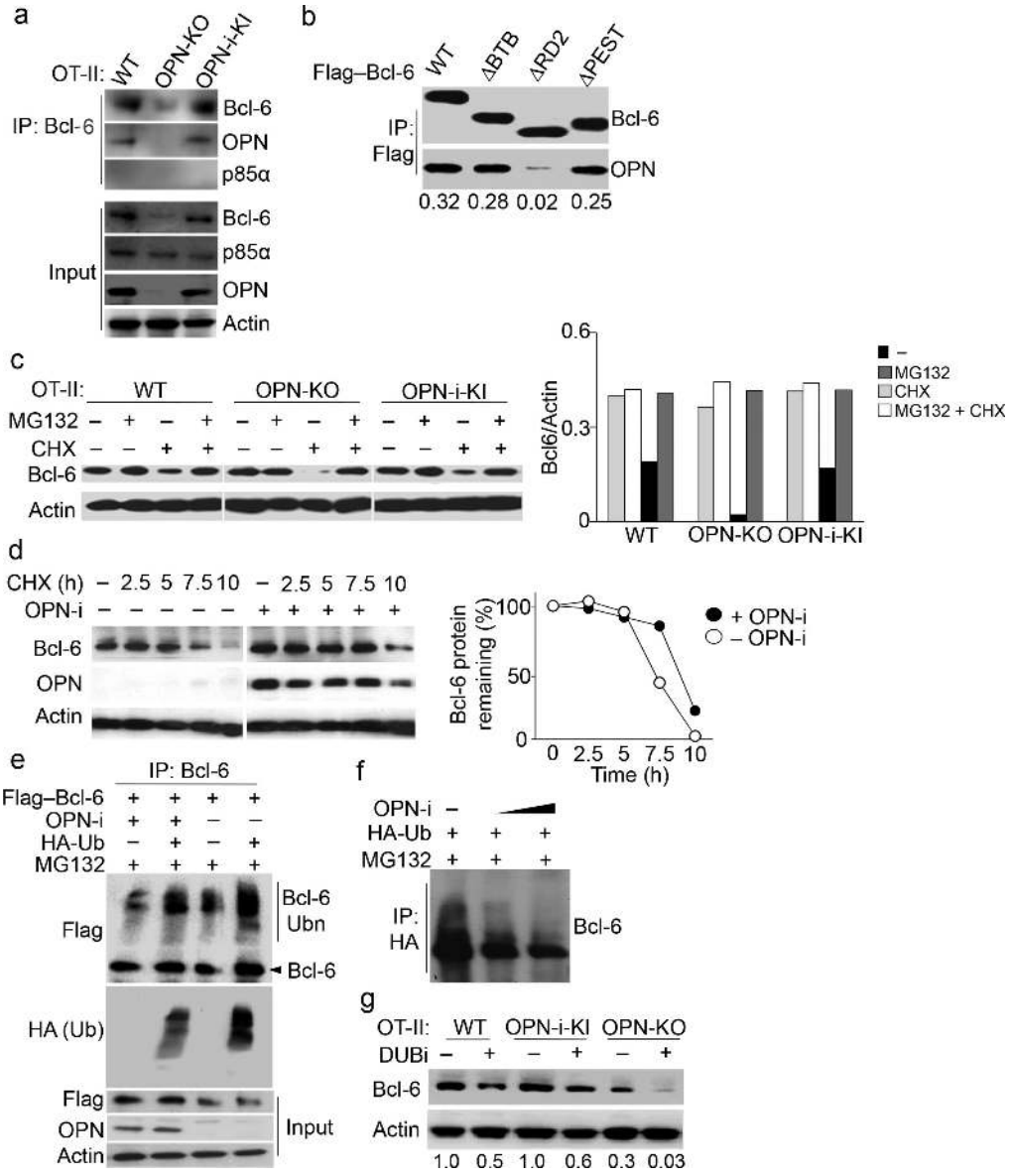

Figure 7.

Intranuclear OPN-i interacts with and stabilizes Bcl-6 expression.

a, Immunoassay of lysates of purified CD44^{+}CD4^{+} T cells from pooled OT-II (n = 8), OT-II OPN-KO (n = 10) and OT-II OPN-i-KI (n = 8) mice 7 d post-immunization with OVA in CFA, assessed by immunoprecipitation (IP) with anti-Bcl-6 and immunoblot analysis, as indicated. **b,** Immunoassay of lysates of 293T cells transfected with plasmids encoding OPN-i and Flag–Bcl-6 wild-type or Flag–Bcl-6 deletion mutants (lanes 1,4,7,10 in Supplementary Fig. 7d), assessed by IP with anti-Flag and immunoblot analysis, as indicated. Bottom, ratios of precipitated OPN to Bcl-6. **c,** Immunoblot analysis of lysates of purified CD62L^{-}CD4^{+} T cells from the indicated OT-II mice 2.5 d post-immunization with OVA in CFA, followed by resting for 2 h, treatment with or without MG132 90 m after incubation with anti-CD3 and anti-ICOS, addition of cycloheximide (CHX) 30 m later, and analysis 3 h after treatment with or without CHX. Right, ratios of Bcl-6 to actin protein. **d,**

Bcl-6 and OPN expression in 293T cells transfected with vectors expressing Flag–Bcl-6 and/or OPN-i, treated with CHX (100 μg/ml) for 10 h. Right, percent of residual Bcl-6 protein relative to that prior to addition of CHX. **e–f**, Immunoassay of lysates of 293T cells transfected with the indicated plasmids and pre-treated with MG132, assessed by denaturation of lysates, IP with anti-Bcl-6 (**e**) or anti-HA (**f**) and immunoblot analysis as indicated. Bcl-6(Ubn): polyubiquitinated Bcl-6. Increasing amounts of OPN-i plasmids in **f. g,** Immunoblot analysis of lysates of purified $CD62L^{-}CD4^{+}$ T cells from indicated OT-II mice 7 d post-immunization with OVA in CFA, treated with (+) or without (−) DUBi for 8 h, probed with anti-Bcl-6 and anti-actin. Bottom, ratios of Bcl-6 to actin. Data represent two (**a–d, g**) and three (**e, f**) independent experiments.

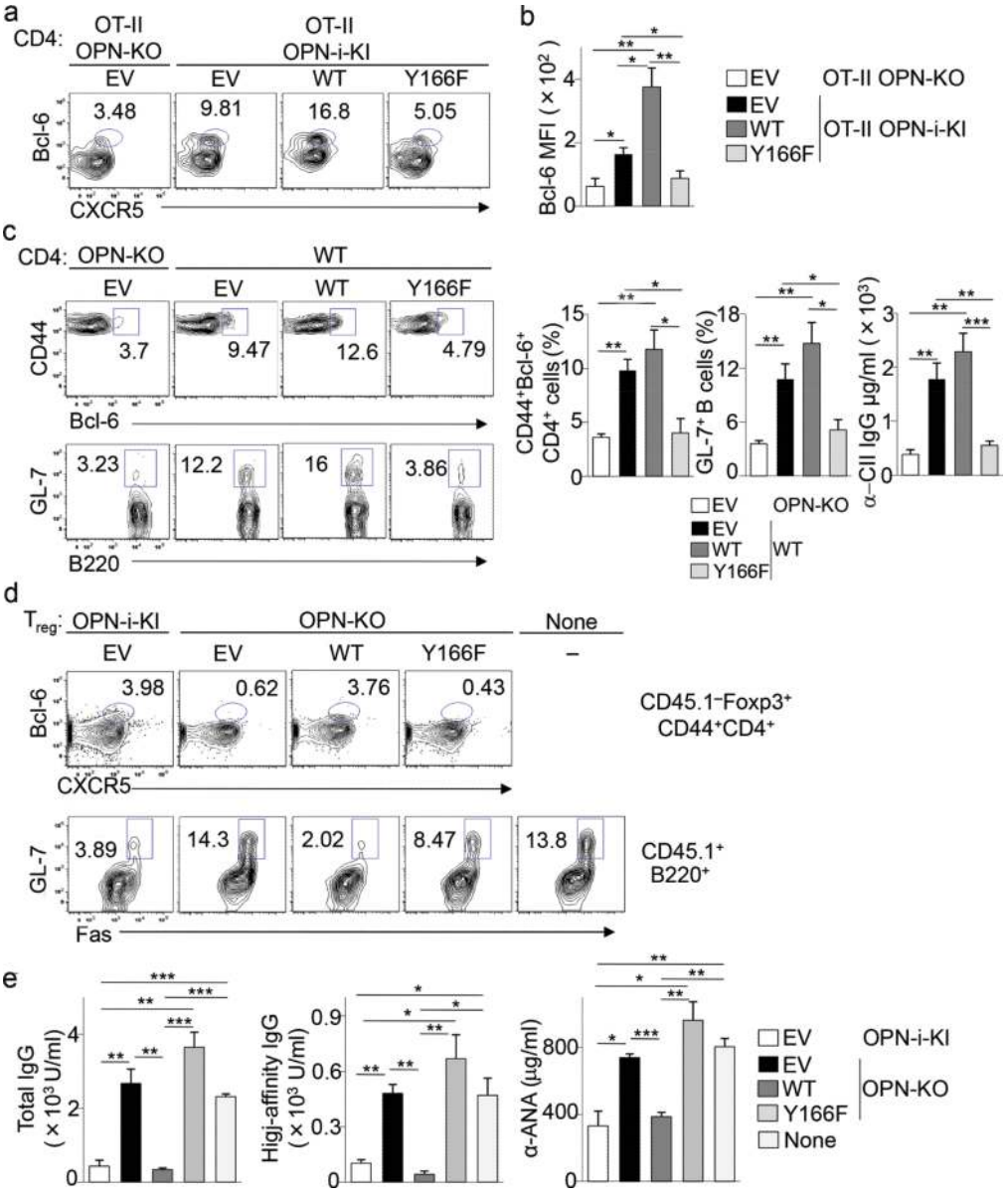

Figure 8.

The p85α–OPN-i interaction regulates T_{FH} and T_{FR} responses *in vivo*.

a, Flow cytometry of donor CD4$^+$ T cells from spleens of *Rag2*$^{-/-}$*Prf1*$^{-/-}$ hosts given OT-II OPN-KO or OT-II OPN-i-KI CD4$^+$ T cells, transduced with retroviral vectors encoding GFP alone (empty vector (EV)) or GFP and OPN-i wild-type or OPN-i Y166F mutant, sorted GFP$^+$ cells and transferred (1×10^5) along with wild-type B cells (1×10^6), rested for 2 d in recipients before immunization with NP_{13}-OVA in CFA and analysis 10 d post-immunization. Numbers indicate percent Foxp3$^-$CXCR5$^+$Bcl-6$^+$ T_{FH} cells. **b,** Bcl-6 protein expression (MFI) in **a** ($n = 5$ per group). **c,** Flow cytometry of spleens of *Rag2*$^{-/-}$*Prf1*$^{-/-}$ hosts given type II collagen (CII)-immune CD4$^+$ T cells from wild-type or OPN-KO mice, transduced with retroviral vectors (as described above), transferred (1×10^5) with wild-type B cells (2×10^6) followed by immunization with CII and CFA at d0 and boosting with CII in

IFA at d21. Right, frequency of Bcl-6$^+$CD44$^+$CD4$^+$ T cells and GL7$^+$B220$^+$ cells, serum titers of anti-mouse CII Ab at d28 (n = 4–6 per group). **d,** Flow cytometry of spleens of *Rag2*$^{-/-}$*Prf1*$^{-/-}$ hosts given CD45.2$^+$ OPN-i-KI or OPN-KO CD25$^+$CD4$^+$ T cells (T_{reg}), transduced with retroviral vectors (as in **a**), transferred sorted GFP$^+$ T cells (4×10^4) together with 1×10^5 CD45.1$^+$ CD25$^-$CD4$^+$ T cells and 2×10^6 wild-type B cells, followed by immunization with NP_{26}-KLH in CFA at d0 and boosting with NP_{26}-KLH in IFA at day 10. Numbers indicate percent CD45.1$^-$Foxp3$^+$Bcl-6$^+$CXCR5$^+$ T_{FR} cells and CD45.1$^+$Fas$^+$GL-7$^+$ GC B cells at d16. **e,** Serum titers of anti-NP and anti-ANA Ab in **d** (n = 3 per group). None: recipients given no T_{reg}. Data represent three (**c**) and two (**a–b, d–e**) independent experiments. *P < 0.05, **P < 0.01 and ***P < 0.001 (unpaired two-tailed Student's t-test; error bars, mean ± s.e.m).